

Luminescence and intersubband excitations in high-density two-dimensional electron gases

H. Peric and B. Jusserand

*Laboratoire de Bagneux, France Telecom, Centre National d'Etudes des Telecommunications,
196 Avenue Henri Ravera, 92220 Bagneux, France*

D. Richards

Cavendish Laboratory, Madingley Road, Cambridge CB3 0HE, England

B. Etienne

Laboratoire de Microstructures et Microélectronique, 196 Avenue Henri Ravera, 92220 Bagneux, France

(Received 28 September 1992)

We report a detailed analysis of both luminescence and electronic Raman-scattering results in modulation-doped single quantum wells. Wave-vector nonconservation in the electron-hole recombination process is demonstrated in these highly doped systems. We also observe, in both polarizations, surprisingly intense Raman lines in addition to the collective excitations of the electron gas. The single-particle character of these lines is proved from the analysis of their dispersion and line shape as a function of the Raman in-plane wave vector.

Modulation-doped structures are of great interest in the study of the quasi-two-dimensional electron gas (2DEG) in both transport and optical experiments, because of the high mobility achieved by separating the electrons from the ionized donors. Among these studies, a large amount of work has been devoted to one-side modulation-doped single quantum wells. This system appears very promising for spectroscopic probes of the integer and fractional quantum Hall effects by optical measurements under a quantizing magnetic field.¹⁻³ The low-temperature photoluminescence spectra of such systems show a broad luminescence line extending from the first conduction-subband edge to the Fermi energy E_F , while the absorption edge is shifted toward E_F because of the phase-space occupation by the 2DEG. This broad line has been attributed to a significant recombination between high-density electrons and localized holes due to acceptor doping⁴ or disorder effects.⁵ Moreover, this relaxation of the k -conservation selection rule has enabled the observation of an enhancement of the luminescence intensity near the Fermi energy E_F .⁵ A sharp Fermi-edge singularity (FES) has also been observed in samples with a near-energetic degeneracy between E_F and the second conduction-subband edge.^{3,6} On the other hand, electronic Raman scattering is a powerful tool for probing electronic excitations, both collective and single particle, occurring in a 2DEG. This was first suggested by Burstein, Pinczuk, and Buchner,⁷ and has since been extensively demonstrated.⁸ From the energetic positions of these excitations, one is able to determine the subband structure as well as the electron density in modulation-doped structures.⁹⁻¹¹ More recently, the observation of distinct spin-density and single-particle excitations, in addition to charge-density waves, opened the way to an independent measure of both direct and exchange-correlation Coulomb interactions of the electron gas.^{12,13} The experimental observation of these different excita-

tions has also made possible a test of the validity of the local-density approximation usually applied to a calculation of the energies of the collective excitations.¹⁴

In this paper, we present both luminescence and electronic Raman-scattering results obtained on the same single asymmetric modulation-doped GaAs quantum wells. We therefore check the consistency of the results of these different optical experiments. In the first part, we report photoluminescence data obtained on two samples with different electron density, and we point out the role of wave-vector nonconservation in the electron-hole recombination process in these highly doped systems. In the second part, we present electronic Raman-scattering spectra of the same samples, where the observation of strong intersubband excitations with a marked in-plane wave-vector dependence is attributed to single-particle excitations (SPE). We further provide a line-shape analysis of this line and discuss its origin.

The two samples each consist of a highly doped 180-Å-thick GaAs single quantum well. A large electron density was obtained by asymmetric modulation doping from a Si δ layer inserted in a $\text{Ga}_{1-x}\text{Al}_x\text{As}$ barrier grown on the top of the structure. The δ layer is separated from the single quantum well by an undoped $\text{Ga}_{1-x}\text{Al}_x\text{As}$ spacer. The density of the 2DEG in the GaAs quantum well is controlled mainly by the thickness of this spacer layer. In the first sample ($S1$), a thickness of 150 Å leads to an electron density around $1 \times 10^{12} \text{ cm}^{-2}$, while in the second sample ($S2$) an electron density around $1.3 \times 10^{12} \text{ cm}^{-2}$ is achieved with a thickness of 100 Å. The experiments were performed in pumped liquid helium (1.8 K), with exciting laser energies around 1.6 eV. Typical incident power lies between 1 and 100 mW, focused onto 1 mm^2 .

The photoluminescence spectra are shown in Fig. 1 for $S1$ and in Fig. 2 for $S2$. In addition to the emission due to bulk GaAs, the photoluminescence (PL) signals exhibit

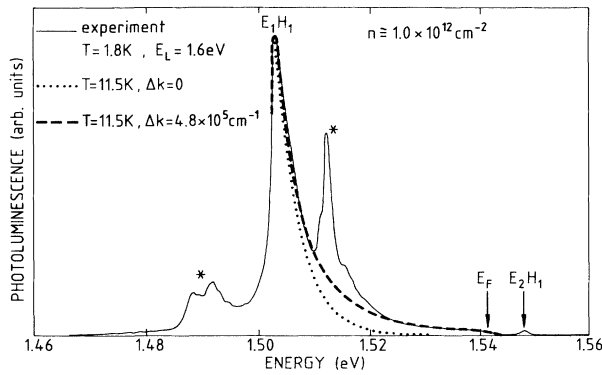


FIG. 1. A comparison between photoluminescence spectra and E_1H_1 line-shape fitting for an n -type GaAs SQW of density $1.10^{12} \text{ cm}^{-2}$ ($S1$). The solid line exhibits the PL signal recorded with a typical power density of 10 W/cm^2 at pumped liquid-He temperature (1.8 K). The dotted line (\cdots) represents a fit of the E_1H_1 line shape considering only vertical transitions ($\Delta k = 0$). The dashed line ($---$) is an E_1H_1 line-shape fit assuming a partial breakdown of the k -conservation selection rule ($\Delta k = 4.8 \times 10^5 \text{ cm}^{-1}$). The peaks labeled by stars are due to the bulk GaAs.

features attributed to the 2DEG. They are very similar in both samples and exhibit two lines.

(i) A broad line, attributed to the E_1 to H_1 transitions between the first conduction and valence subbands of the well. Its peak positions, 1.5067 eV in $S1$ and 1.5039 eV in $S2$, lie below the bulk GaAs band gap because of the electric field due to the large electron density in the quantum well (QW). This line displays a high-energy tail extending over 50 meV up to the Fermi energy E_F , because of the large population of the first conduction subband E_1 .

(ii) A narrow peak, at 1.5503 eV in $S1$ and 1.5523 eV in $S2$, attributed to the E_2 to H_1 transitions between the second conduction subband and the first heavy-hole subband.

We notice that the intensity of this line is smaller than the E_1H_1 one under weak excitation ($< 20 \text{ mW}$), but becomes comparable or larger under strong excitation ($>$

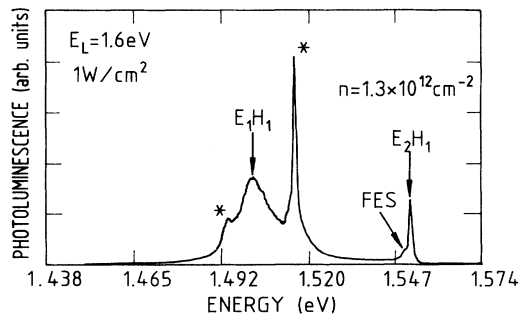


FIG. 2. The PL signal for the sample of higher density $1.3 \times 10^{12} \text{ cm}^{-2}$ ($S2$) recorded with a laser energy of 1.6 eV and a power density of 1 W/cm^2 . The peaks labeled by stars are due to the bulk GaAs. The lines coming from the 2DEG are labeled E_1H_1 and E_2H_1 , respectively, while FES refers to the Fermi singularity.

50 mW). However, this line remains narrow whatever the incident power density, suggesting that the second electronic subband is not significantly populated even under strong excitation. This is further demonstrated by photoluminescence excitation spectra, which show two sharp and intense lines, respectively attributed to E_2H_1 and E_2L_1 excitonic transitions: no significant shift is observed between E_2H_1 lines as observed by PL and photoluminescence excitation (PLE). Therefore electronic Raman-scattering experiments, which require very high power excitation (200 mW) because of the weak cross section, will not lead to a significant population of E_2 . From the positions of the E_1H_1 and E_2H_1 peaks, we can estimate the distance between the two conduction subbands $E_2 - E_1$. We find 43.6 and 48.4 meV for $S1$ and $S2$, respectively. In the second part of the paper, these values will be compared to electronic Raman experiments which allow a direct determination of $E_2 - E_1$.

Let us first analyze the E_1H_1 line shape. In both samples, the luminescence intensity of this line regularly decreases from the band gap to the Fermi energy E_F . In $S1$, where the Fermi edge is far enough from the E_2H_1 excitonic transition, the PL signal (see Fig. 1) exhibits a clear falloff at this energy. On the contrary, in $S2$ the Fermi energy lies very close to the E_2H_1 excitonic transition, and a shoulder appears on the lower side of this transition (see Fig. 2). This feature has already been reported in similar samples under very weak excitation by Chen *et al.*, and attributed to a Fermi-edge singularity, strongly enhanced because of the near-energetic degeneracy between E_F and E_2 .^{3,6} However, in our sample the structure close to E_2H_1 is still observable under strong excitation power density ($> 5 \text{ W/cm}^2$) and should be related to another mechanism. In what follows, we do not consider many-body effects, and use a simple model of band-to-band recombination to reproduce the E_1H_1 line shape.

With the typical incident power density in our experiments, the recombination process only involves near-zone-center photocreated holes in the HH_1 subband. We first assume a strict conservation of the wave vector during the recombination process, and fit the carrier temperature. We assume that electrons and holes are thermalized at the same temperature $T_e = T_h = T$ and obtain $T = 11.5 \text{ K}$ for $S1$ and $T = 20 \text{ K}$ for $S2$. As shown in Fig. 1 (dotted line) for $S1$, this model reproduces well the low-energy part of the E_1H_1 line, but is unable to account for the falloff in amplitude near E_F . Therefore we partly relax the usual k -conservation selection rule using a phenomenological Lorentzian broadening Δk . This distribution for the change in k gives a nonvanishing probability for all electrons in the Fermi sea to recombine with $k \approx 0$ holes. The line shape obtained in this model is shown in Fig. 1 (dashed line) for $S1$, and well reproduces the sudden falloff in amplitude near E_F . The best fit gives a carrier temperature of $T = 11.5 \text{ K}$ and a broadening parameter $\Delta k = 4.8 \times 10^5 \text{ cm}^{-1}$. The fit for $S2$ is also in very good agreement with experiments, if one neglects the shoulder close to E_2H_1 , as assumed above. The fit parameters are $T = 15 \text{ K}$ and $\Delta k = 1.3 \times 10^6 \text{ cm}^{-1}$.

Such broadening has been already observed in $\text{In}_x\text{Ga}_{1-x}\text{As-InP}$ quantum wells and attributed to disorder effects in the QW due to alloy fluctuations.⁵ These effects lead to hole localization, resulting in the breakdown of the k -conservation selection rule. Broad luminescence lines, attributed to the localization of holes, have also been observed in modulation-doped samples with slight acceptor doping in the quantum well.^{4,15} In our samples, where disorder is minimized in the GaAs QW's, we can explain the comparatively weak but significant high-energy tail of the E_1H_1 line by considering a partial relaxation of the k -conservation selection rule, modeled by a phenomenological broadening Δk . This could be attributed to Coulombic interactions between the ionized remote donors in the $\text{Ga}_{1-x}\text{Al}_x\text{As}$ barrier and the 2DEG, or more likely to defect scattering at the rough inverted interface. Because of the self-consistent electric field, holes wave functions indeed are predominantly located at this interface. This phenomenon increases with the electron density in the well, in agreement with the fitted Δk values.

Let us now present the intersubband Raman-scattering results on the same samples. Here we concentrate our attention on the Raman-scattering signal associated with the transitions from filled states below E_F , inside the lowest conduction subband E_1 , toward empty states in the first excited subband E_2 . Intraband signals from sample $S2$ have been previously reported.¹⁶ Raman-scattering experiments were also done at liquid-helium temperature (1.8 K) and under close energy resonance with the fundamental energy gap.

Figure 3 shows electronic intersubband Raman spectra obtained in $S2$ in parallel (polarized spectra) and crossed (depolarized spectra) polarizations, respectively, for two different Raman in-plane wave vectors: $q_{\parallel} \approx 0$ (the left side of the figure) and $q_{\parallel} \approx 1.5 \times 10^5 \text{ cm}^{-1}$ (the right-hand side of the figure). In the backscattering setup, we can

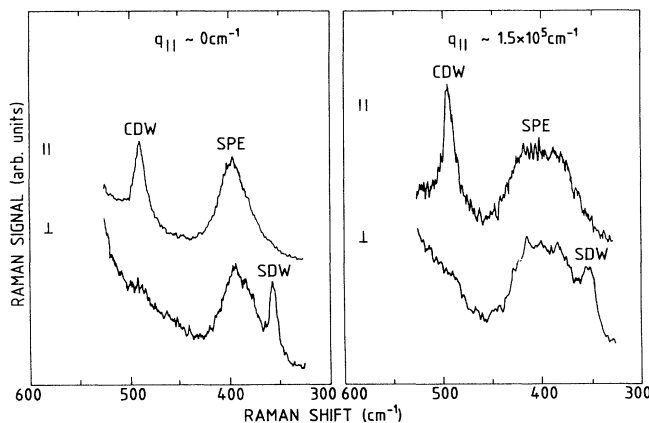


FIG. 3. Electronic Raman-scattering spectra of $S2$ obtained with a resonance laser energy of 1.64 eV and at pumped liquid-He temperature (1.8 K). The left-hand side of the figure shows collective (CDW and SDW) and individual (SPE) intersubband excitations of the 2DEG for a very small Raman in-plane wave vector, while the right-hand side exhibits the same excitations at larger q_{\parallel} .

change q_{\parallel} in the plane of the 2DEG by simply rotating the sample relative to the fixed incident light wave vector. Charge-density excitations occur in polarized spectra, while spin-density excitations are active in depolarized spectra. The sharp lines with well-defined polarization selection rules are assigned, respectively, to collective charge-density waves (CDW's) and spin-density waves (SDW's) occurring in the 2DEG. We also observe, in both polarizations, a broader band labeled SPE, with an intensity comparable to the collective ones. It is located at the same energy (395 cm^{-1}) for both polarizations; this energy is very close to the intersubband energy $E_2 - E_1$. Moreover, this band displays a specific behavior as a function of q_{\parallel} . Unlike the CDW and SDW, which remain approximately unchanged, the SPE band is strongly broadened with increasing Raman in-plane wave vector. At large q_{\parallel} , the shape of this line is nearly rectangular and symmetrical within experimental accuracy. An experimental dispersion curve of all excitations, shown in Fig. 4, is deduced from a systematic study as a function of the angular configuration. The CDW and SDW lines are not strongly dispersive because of their large shift from the single-particle transitions. On the contrary, we observe a continuous broadening of the SPE line with increasing q_{\parallel} . Such wave-vector dependence is typical of nonvertical single-particle intersubband transitions between the two lowest conduction subbands E_1

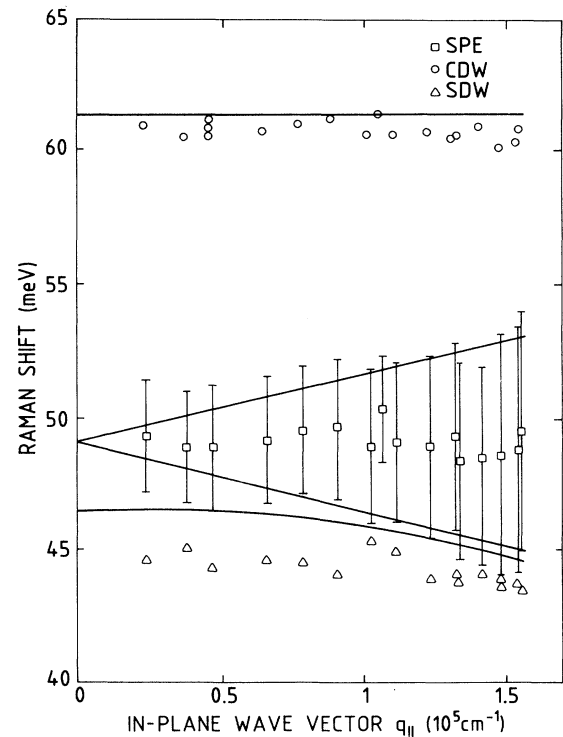


FIG. 4. The dispersion curve of the collective (CDW and SDW) and individual (SPE) intersubband excitations of the 2DEG, deduced from Raman-scattering experiments as a function of q_{\parallel} . The vertical lines are the width at half maximum of the SPE line. The experimental curves are compared to the calculated ones (solid lines) as explained in the text.

and E_2 . They cover a continuum bounded by the $E_{12} \pm \hbar q_{\parallel} v_F$ curves, where v_F is the Fermi velocity and E_{12} is the subband spacing at $q_{\parallel} = 0$.

This intersubband SPE signal appears to be very intense and well defined in this highly doped sample as compared to previous observations.^{12–14} This is in contradiction to the expected complete screening of the SPE due to collective effects.⁸

The extrapolation to the zone center of the intersubband SPE dispersion provides a determination of the subband splitting $E_2 - E_1$, here about 49 meV. This value is in very good agreement with the PL estimation (48.4 meV) reported above. In *S1*, we obtain the same overall behavior of the Raman spectrum, and a similarly good agreement between luminescence and SPE data. Let us now model the SPE line shape of the E_1 to E_2 intersubband transition. The model is based on a numerical integration over the Fermi disk of the usual intersubband Lindhard polarizability for a noninteracting electron gas:

$$\chi_0^{nn'}(q_{\parallel}, \omega) = \frac{1}{\Omega} \int_0^{k_F} \frac{f_0(E_{\mathbf{k}+q_{\parallel}}^{n'}) - f_0(E_{\mathbf{k}}^n)}{E_{\mathbf{k}+q_{\parallel}}^{n'} - E_{\mathbf{k}}^n - \hbar\omega} d^2\mathbf{k},$$

where f_0 is the Fermi-Dirac distribution, $E_{\mathbf{k}+q_{\parallel}}^{n'}$ the dispersion relation of the final state, while $E_{\mathbf{k}}^n$ refers to the initial state. The Raman cross section associated with the intersubband transition is then proportional to

$$R^{nn'}(\omega, q_{\parallel}) \approx n(\omega) \chi_0^{nn'}(q_{\parallel}, \omega),$$

where $n(\omega)$ is the Bose-Einstein factor population. In this expression, a perfect conservation of the wave vector is assumed.

Using a temperature of 5 K, we are unable to reproduce the experimental line shape of the SPE whatever the Raman in-plane wave vector. Increasing the temperature up to 30 K allows us to reproduce the flat shape of the SPE line at large wave vector, because of the thermal population in E_2 near the zone center. However, this procedure, applied at small q_{\parallel} , does not give a good agreement with the experiments. Moreover, this temperature is surprisingly high when compared to the carrier temperature estimated by the luminescence line-shape analysis. Therefore, we introduce in the Raman process, as we did for the luminescence process, a breakdown of the k -conservation selection rule to model the SPE band. Taking a very small Raman in-plane wave vector, the dispersion effects are negligible, and the line-shape broadening is dominated by disorder. Assuming a Lorentzian broadening of width $\Delta k = 1.5 \times 10^5 \text{ cm}^{-1}$, we obtain a SPE linewidth of 4 meV, in good agreement with our experimental data at small q_{\parallel} . This value is several times smaller than the one obtained in the luminescence spectra. This difference is not surprising because the luminescence broadening, contrary to the Raman-scattering one, is controlled mainly by hole localization effects.

In conclusion, the wave-vector dependence of the SPE line, as well as its line shape, allow us to definitely assign this line to single-particle intersubband excitations between the two lowest conduction subbands. However, a discrepancy remains in the quantitative modeling of the line shape at large wave vector, even assuming a wave-vector broadening. This should be improved by using energy-dependent broadening in the degenerate conduction band.^{17,18}

In our samples, the SPE lines are well separated from the CDW and SDW lines. Thus one is able to accurately determine their energies, and to deduce the electron density. Using a random-phase-approximation (RPA) calculation based on self-consistently determined wave functions,^{9,13} we deduce from the CDW energy an electron density of $1.3 \times 10^{12} \text{ cm}^{-2}$. With this value, one may extract from self-consistent subband calculations the potential profile of the structure and the subband energies. The calculated value of the $E_1 - E_2$ intersubband energy obtained by this procedure is in very good agreement with experimental values provided by PL (48.4-meV) and Raman (49-meV) measurements. Moreover, from the experimental SPE, CDW, and SDW lines, one may extract an experimental determination of the direct and exchange-correlation Coulomb interaction, $2n\alpha$ and $2n\beta$, respectively.^{12–14} The ratio β/α accounts for the relative strength of the exchange-correlation and direct Coulomb interactions; it is found to be equal to 0.27 and 0.26 for *S1* and *S2*, respectively. These values show that these interactions have comparable strengths in this high-density 2DEG. This is consistent with previous estimations performed on samples with lower densities.^{12–14} In Fig. 4, we show (solid lines) the calculated CDW and SDW dispersions, as well as the calculated SPE width dispersion. The SDW energies have been determined using a parametrization for the exchange-correlation potential within the local-spin-density approximation (LSDA).^{13,14,19} As has been shown for lower-density samples, the LSDA is found to underestimate the magnitude of the exchange-correlation interaction.¹⁴ However, the general trend of all the experimental dispersions is correctly reproduced.

In conclusion, we have obtained an excellent understanding of the optical properties of the 2DEG, thanks to the combination of PL and electronic Raman-scattering experiments. The E_1H_1 luminescence line-shape analysis gives evidence of the partial breakdown of the k -conservation selection rule in the PL process of these highly doped systems. On the other hand, electronic Raman-scattering experiments have allowed us to study collective as well as single-particle excitations of the 2DEG. The very good agreement for the intersubband energy $E_2 - E_1$, obtained by PL (48.4 meV) and Raman-scattering experiments (49 meV), is a strong indication of the single-particle nature attributed to the SPE line. Moreover, we have shown that the SPE linewidth had a marked dependence with q_{\parallel} , proving its single-particle character. This was further demonstrated from a line-shape analysis including some breakdown of the wave-vector conservation. However, some disagreement remains for the modeling at large q_{\parallel} . Our observation of

SPE lines with an intensity comparable to that of the collective ones in both polarizations disagrees with the usual Raman processes and is still not very well understood. Finally we showed that direct and exchange-correlation Coulomb interactions have comparable strengths in a high-density 2DEG.

The authors acknowledge J. Y. Marzin, C. Tanguy, and B. Sermage for many helpful discussions and a critical reading of the manuscript. The Laboratoire de Bagneux and Laboratoire de Microstructures et Microélectronique are unites associées au Centre National de la Recherche Scientifique.

-
- ¹B. B. Goldberg, D. Heiman, A. Pinczuk, L. Pfeiffer, and K. West, *Phys. Rev. Lett.* **65**, 641 (1990).
- ²A. J. Turberfield *et al.*, *Phys. Rev. Lett.* **65**, 637 (1990).
- ³W. Chen, M. Fritze, A. V. Nurmikko, C. Colvard, D. Ackley, and H. Lee, *Phys. Rev. Lett.* **64**, 2434 (1990).
- ⁴I. F. Kukushin and V. B. Timofeev, *Pis'ma Zh. Eksp. Teor. Fiz.* **40**, 413 (1984) [*JETP Lett.* **40**, 1232 (1984)].
- ⁵M. S. Skolnick, J. M. Rorison, K. J. Nash, D. J. Mowbray, P. R. Tapster, S. J. Bass, and A. D. Pitt, *Phys. Rev. Lett.* **58**, 2130 (1987).
- ⁶W. Chen, M. Fritze, A. V. Nurmikko, M. Hong, and L. L. Chang, *Phys. Rev. B* **43**, 14 738 (1991).
- ⁷E. Burstein, A. Pinczuk, and S. Buchner, in *Physics of Semiconductors*, edited by B. L. H. Wilson, IOP Conf. Proc. No. 43 (Institute of Physics and Physical Society, London, 1979), p. 1231.
- ⁸A. Pinczuk and G. Abstreiter, in *Light Scattering in Solids V*, edited by M. Cardona and G. Güntherodt (Springer, Heidelberg, 1988), p. 153.
- ⁹G. Fasol, R. D. King-Smith, D. Richards, U. Ekenberg, N. Mestres, and K. Ploog, *Phys. Rev. B* **39**, 12 695 (1989).
- ¹⁰B. Jusserand, D. R. Richards, G. Fasol, G. Wiemann, and W. Schlapp, *Surf. Sci.* **229**, 394 (1990).
- ¹¹D. Richards, G. Fasol, and K. Ploog, *Appl. Phys. Lett.* **57**, 1099 (1990).
- ¹²A. Pinczuk, S. Schmitt-Rink, G. Danan, J. P. Valladares, L. N. Pfeiffer, and K. W. West, *Phys. Rev. Lett.* **63**, 1633 (1989).
- ¹³D. Gammon, B. V. Shanabrook, J. C. Ryan, and D. S. Katzer, *Phys. Rev. B* **41**, 12 311 (1990).
- ¹⁴D. Gammon, B. V. Shanabrook, J. C. Ryan, D. S. Katzer, and M. J. Yang, *Phys. Rev. Lett.* **68**, 1884 (1992).
- ¹⁵R. Cingolani, Y. H. Zhang, R. Rinaldi, M. Ferrara, and K. Ploog, *Surf. Sci.* **267**, 457 (1992).
- ¹⁶B. Jusserand, D. Richards, B. Etienne, H. Peric, and G. Fasol, *Surf. Sci.* **263**, 527 (1992); B. Jusserand, D. Richards, H. Peric, and B. Etienne, *Phys. Rev. Lett.* **69**, 848 (1992).
- ¹⁷P. T. Landsberg, *Phys. Status Solidi* **15**, 623 (1966); R. W. Martin and H. L. Störmer, *Solid State Commun.* **22**, 523 (1977).
- ¹⁸S. K. Lyo and E. D. Jones, *Phys. Rev. B* **38**, 4113 (1988).
- ¹⁹O. Gunnarsson and B. T. Lundqvist, *Phys. Rev. B* **13**, 4274 (1976).